A study of the $B^0 \to K^0_S \pi^0$ decay at Belle II

S. Hazra

(On behalf of the Belle II Collaboration)

Tata Institute of Fundamental Research, Mumbai 400 005, India
sagar.hazra@tifr.res.in

Abstract. The decay $B^0 \to K^0_S \pi^0$ proceeds via $b \to s$ loop diagrams. Such flavour changing neutral current transitions are highly suppressed in the standard model and provide an indirect route to search for new physics. In particular, the expected large yield of this charmless decay at Belle II will allow us to precisely measure the *CP* violation asymmetry. We report herein preliminary results based on a simulation sample.

Keywords: CPV

1 Introduction

In the standard model (SM), the decay $B^0 \to K^0_S \pi^0$ proceeds via $b \to s$ loop diagrams [1]. Such flavour changing neutral current transitions are highly suppressed and provide an important route to indirectly search for new physics by checking the consistency between measurements and corresponding theory predictions as new particles may enter the quantum loop [1]. Within the SM, *CP* violation (CPV) arises due to a single irreducible phase in the Cabibbo-Kobayashi-Maskawa (CKM) matrix [2]. At a flavor-factory experiment such as Belle II, neutral B meson pairs are coherently produced in the process $\Upsilon(4S) \to B^0\bar{B}^0$. When one of these B mesons decays to a *CP* eigenstate f_{CP} and the other to a flavor-specific final state $f_{\rm tag}$, the time-dependent decay rate is given as

$$\mathcal{P}(\Delta t) = \frac{e^{-|\Delta t|/\tau_{B^0}}}{4\tau_{B^0}}[1 + q\{\mathcal{A}\cos(\Delta m_d \Delta t) + \mathcal{S}\sin(\Delta m_d \Delta t)\}], \qquad (1)$$

where $\Delta t = t_{CP} - t_{\rm tag}$ is the proper decay time difference between f_{CP} and $f_{\rm tag}$, $q = \pm 1$ is the flavor of $f_{\rm tag}$ being $+1$ (-1) for B^0 $(\bar{B}^0)$ decaying to $f_{\rm tag}$, Δm_d is the B^0-$\bar{B}^0$ mixing frequency, and τ_{B^0} is the B^0 lifetime. The quantity $\mathcal{A}$ is a measure of direct CPV and $\mathcal{S}$ denotes CPV due to interference between decays with and without $B\bar{B}$ mixing. The key challenge in performing a time-dependent *CP* analysis for $B^0 \to K^0_S \pi^0$ arises due to the absence of primary charged final-state particles at the B decay vertex. Instead, we calculate Δt as $(z_{\rm rec} - z_{\rm tag})/\beta\gamma c$, where $\beta\gamma$ is the Lorentz boost, $z_{\rm rec}$ is the z position of the B vertex reconstructed from the intersection of the K^0_S trajectory with the interaction region, and $z_{\rm tag}$ is calculated using the remaining tracks.

The CKM and color suppression of the tree-level $b \to su\bar{u}$ transition means that the $B^0 \to K^0_S\pi^0$ decay is dominated by the top-quark mediated $b \to sd\bar{d}$ loop diagram, which carries a weak phase $\arg(V_{tb}V^*_{ts})$. Here V_{ij} are the CKM matrix elements. If subleading contributions are small, $\mathcal{S}_{K^0_S\pi^0}$ is expected to be equal to $\sin(2\phi_1)$ and $\mathcal{A}_{K^0_S\pi^0} \approx 0$. Therefore, a precise measurement of the direct *CP* asymmetry and branching fraction in this decay channel represents an important consistency test of the SM. With the data size anticipated at Belle II, we expect to have significantly smaller uncertainties compared to what Belle [3, 4] and BaBar [5, 6] have achieved for these quantities.

2 Event sample and selection

We use 7×10^5 $B^0\bar{B}^0$ Monte Carlo (MC) events for the signal study. We also use $e^+e^- \to u\bar{u}$, $d\bar{d}$, $c\bar{c}$, $s\bar{s}$, $B^0\bar{B}^0$ and B^+B^- MC events, each equivalent to an integrated luminosity of $400\,\mathrm{fb}^{-1}$, to identify backgrounds. The MC events are simulated with the geometry and background condition for the Belle II detector [7] at SuperKEKB. The detector elements relevant to reconstruct the $B^0 \to K^0_S\pi^0$ decay are the vertexing and tracking system as well as the electromagnetic calorimeter.

A K^0_S candidate is reconstructed in its $\pi^+\pi^-$ decay by requiring the reconstructed invariant mass to lie between 482 and $513\,\mathrm{MeV}/c^2$, which corresponds to a $\pm 6\sigma$ window around the nominal K^0_S mass, where σ is the invariant-mass resolution. To reconstruct $\pi^0 \to \gamma\gamma$ candidates, we apply a photon energy threshold of 30, 60, and 80 MeV for the barrel, backward and forward endcap region, respectively, of the calorimeter. We require the reconstructed π^0 mass to lie between 120 and $145\,\mathrm{MeV}/c^2$. We also require the magnitude of the cosine of the π^0 helicity angle to be less than 0.98; this helps suppress misreconstructed π^0 candidates.

B-meson candidates are reconstructed by combining K^0_S and π^0 candidates. For this purpose, we use two kinematic variables, namely the beam-energy-constrained mass (M_{bc}) and the energy difference (ΔE), defined as

$$\begin{aligned} M_{\mathrm{bc}} &= \sqrt{E^2_{\mathrm{beam}} - \vec{p}^{\,2}_B}, \\ \Delta E &= E_B - E_{\mathrm{beam}}, \end{aligned} \tag{2}$$

where E_{beam} is the beam energy, E_B and $\vec{p}_B$ are the reconstructed energy and momentum of the B meson respectively, all calculated in the center-of-mass frame. We retain candidate events satisfying the following criteria: $|\Delta E| < 0.3\,\mathrm{GeV}$ and $5.24 < M_{\mathrm{bc}} < 5.29\,\mathrm{GeV}/c^2$.

The dominant source of backgrounds in this analysis comes from $e^+e^- \to q\bar{q}$ ($q = u$, d, s or c) continuum process. This background is suppressed by exploiting the difference in event topology. Continuum events result in final-state particles collimated into two back-to-back jets, whereas the final-state particles from $e^+e^- \to \Upsilon(4S) \to B\bar{B}$ are uniformly distributed over the 4π solid angle. We use a boosted decision tree (BDT) [8] classifier to combine event-shape variables

and apply a criterion on the BDT output by maximising the signal significance. Figure 1 shows $M_{\rm bc}$ and ΔE distributions obtained after the continuum suppression requirement is applied.

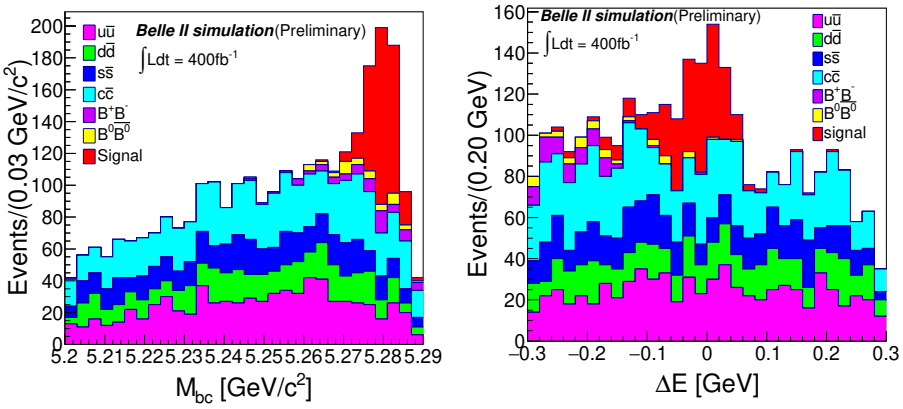

Fig. 1: $M_{\rm bc}$ and ΔE distributions obtained after the continuum suppression.

3 Signal yield extraction

To extract the signal yield, we use an extended unbinned maximum-liklihood fit to the two-dimensional distribution of $M_{\rm bc}$ and ΔE. As the signal $M_{\rm bc}$ is correlated with ΔE, we reduce the correlation by using the modified $M_{\rm bc}$ introduced in Ref. [9]. We can now consider the product of two individual probability density functions (PDFs) to be a good approximation for the total PDF. The extended likelihood function is given as

$$\mathcal{L} = \frac{e^{-\sum_j n_j}}{N!} \prod_i^N \left[\sum_j n_j \mathcal{P}_j^i \right], \tag{3}$$

where N is the total number of candidate events, n_j is the yield of event category j, and $\mathcal{P}_j^i$ is the PDF of the same category for event i. Table 1 lists various PDFs used to model the $M_{\rm bc}$ and ΔE distributions. We fix the yield and PDF shape of the $B\bar{B}$ background category in the fit.

Figure 2 shows the $M_{\rm bc}$ and ΔE projections of the fit. In Table 2 we compare the fitted yields of signal and $q\bar{q}$ background with their expected values.

4 Summary

The $B^0 \to K^0_S \pi^0$ decay constitutes an important channel at Belle II for the precise measurement of time-dependent CP asymmetry, as well as its branching

Table 1: List of PDFs used to model $M_{\rm bc}$ and ΔE distributions.

Event category	$M_{\rm bc}$	ΔE
Signal	Crystal Ball [10] + Gaussian	Double-sided Crystal Ball + Gaussian
$B\bar{B}$	Two-dimensional kernel estimation PDF [11]	
$q\bar{q}$	ARGUS [12]	Chebyshev polynomial

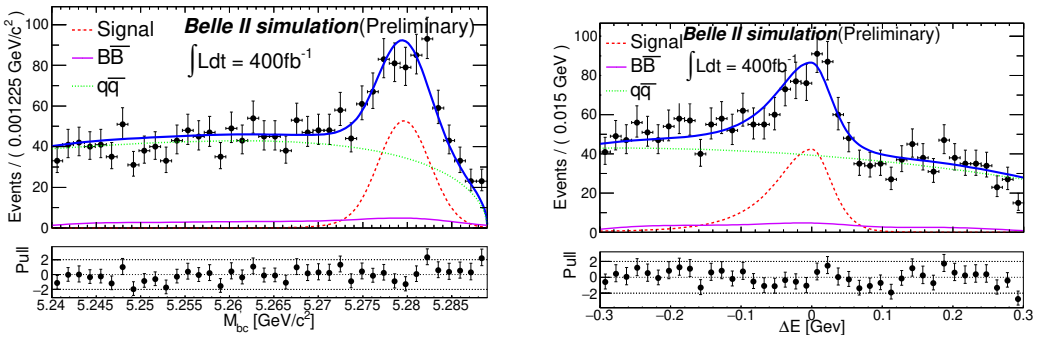

Fig. 2: Projections of $M_{\rm bc}$ and ΔE obtained with the maximum-likelihood fit.

Table 2: Expected and fitted yield for signal and $q\bar{q}$ background.

Category	Expected yield	Fitted yield
Signal	317	316 ± 32
$q\bar{q}$	1519	1499 ± 47

fraction. We have deployed a multivariate analysis method to suppress backgrounds and performed an unbinned maximum-liklihood fit to extract the signal yield. We are now developing a time-dependent CPV analysis framework.

References

1. E. Kou et et al. (Belle II Collaboration), PTEP **2019** no. 12, 123C01 (2019).
2. N. Cabibbo, Phys. Rev. Lett. **10**, 531 (1963); M. Kobayashi and T. Maskawa, Prog. Theor. Phys. **49**, 652 (1973).
3. Y. Chao et al. (Belle Collaboration), Phys. Rev. D **69**, 111102 (2004).
4. K. F. Chen et al. (Belle Collaboration), Phys. Rev. D **72**, 012004 (2005).
5. B. Aubert et al. (BaBar Collaboration), Phys. Rev. Lett. **93**, 131805 (2004).
6. B. Aubert et al. (BaBar Collaboration), Phys. Rev. D **71**, 111102 (2005).
7. T. Abe *et al.*, arXiv:1011.0352 (2010).
8. T. Keck et al., arXiv:1609.06119 (2016).
9. See Section 7.1.1.2 of A. Bevan et al., Eur. Phys. J. C **74**, 3026 (2014).
10. T. Skwarnicki, A study of the radiative cascade transitions between the Upsilon-prime and Upsilon resonances, PhD thesis, Institute of Nuclear Physics, Krakow, 1986, DESY-F31-86-02.
11. K. S. Cranmer, Comput. Phys. Commun. **136** (2001) 198-207.
12. H. Albrecht et al. (ARGUS Collaboration), Phys. Lett. B **241**, 278 (1990).